Chinese Journal of Natural Medicines

The ethyl acetate extract of *Schefflera kwangsiensis* ameliorates oxaliplatin-induced peripheral neuropathic pain *via* SERCA2b

Jie Li, Xihua Li, Ying Chen, Wumei Wang, Xuesong Chen, Chunlei Zhang, Zhengyu Cao, Fang Zhao

Citation: Jie Li, Xihua Li, Ying Chen, Wumei Wang, Xuesong Chen, Chunlei Zhang, Zhengyu Cao, Fang Zhao, The ethyl acetate extract of *Schefflera kwangsiensis* ameliorates oxaliplatin-induced peripheral neuropathic pain *via* SERCA2b, Chinese Journal of Natural Medicines, 2026, 24(3), 326-337. doi: 10.1016/S1875-5364(26)61107-7.

View online: https://doi.org/10.1016/S1875-5364(26)61107-7

Chinese Journal of Natural Medicines 24 (2026) 326-337

Contents lists available at ScienceDirect

Chinese Journal of Natural Medicines

journal homepage: www.cjnmcpu.com/

Original article

The ethyl acetate extract of *Schefflera kwangsiensis* ameliorates oxaliplatin-induced peripheral neuropathic pain *via* SERCA2b

Jie Li[a,Δ], Xihua Li[a,Δ], Ying Chen[a, b, c], Wumei Wang[d], Xuesong Chen[e], Chunlei Zhang[a], Zhengyu Cao[a,*], Fang Zhao[a, b,*]

[a] *State Key Laboratory of Natural Medicines and Jiangsu Provincial Key Laboratory for TCM Evaluation and Translational Development, School of Traditional Chinese Pharmacy, China Pharmaceutical University, Nanjing 211198, China*

[b] *State Key Laboratory on Technologies for Chinese Medicine Pharmaceutical Process Control and Intelligent Manufacture, Jiangning Industrial City, Economic and Technological Development Zone of Lianyungang, Lianyungang 222001, China*

[c] *Jiangsu Kanion Pharmaceutical Co. Ltd., Jiangning Industrial City, Economic and Technological Development Zone of Lianyungang, Lianyungang 222001, China*

[d] *The School of Ecology and Environment, Tibet University, Lhasa 850000, China*

[e] *The first Affiliated Hospital of Nanjing Medical University, Nanjing 210029, China*

ARTICLE INFO

Article history:
Received 23 February 2025
Revised 11 June 2025
Accepted 17 June 2025
Available online 20 April 2026

Keywords:
Oxaliplatin-induced peripheral neuropathy
Neuropathic pain
Sarco/endoplasmic reticulum Ca^{2+}-ATPase
Schefflera kwangsiensis

ABSTRACT

Oxaliplatin (OXA) is a widely used chemotherapeutic agent whose clinical utility is limited by OXA-induced peripheral neuropathy (OIPN). Sarco/endoplasmic reticulum Ca^{2+}-ATPase (SERCA) transports Ca^{2+} from the cytoplasm into the endoplasmic reticulum (ER), thereby maintaining intracellular Ca^{2+} homeostasis. *Schefflera kwangsiensis* Merr. ex H.L. Li (SKM) is traditionally used to treat neuropathic pain conditions such as trigeminal neuralgia and sciatica, and its active component Schekwanglupaside C has been identified as a potent SERCA activator. In this study, an OIPN mouse model was established by intraperitoneal administration of OXA (4 mg·kg^{-1}) on days 1, 2, 8, 9, 15, and 16. SERCA2b mRNA and protein expression in dorsal root ganglia (DRG) were evaluated by quantitative polymerase chain reaction (qPCR) and immunofluorescence. Mechanical allodynia was assessed using the Von Frey test. DRG neuronal excitability was examined by whole-cell current-clamp recordings, whereas oxidative stress and neuronal apoptosis/necrosis were assessed using the reactive oxygen species (ROS)-sensitive probe 2',7'-dichlorofluorescin diacetate (H_2DCFDA) and fluorescein isothiocyanate (FITC)/propidium iodide (PI) dual staining. This study identifies SERCA2b as a novel therapeutic target for OIPN. We observed that SERCA2b mRNA and protein levels were significantly downregulated during OIPN progression. Treatment with the SERCA agonist CDN1163 (CDN), the ethyl acetate extract of SKM (SKM.Ext), or duloxetine (DLX) attenuated neuronal pathology, restored DRG neuron soma diameter, and reduced the expression of pro-inflammatory cytokines interleukin-1β (IL-1β) and tumor necrosis factor α (TNF-α). Pre-incubation of DRG neurons with CDN1163 or SKM.Ext for 1 h significantly attenuated OXA-induced hyperexcitability and reduced the abnormal increase in voltage-gated sodium channel (VGSC) current density. Inhibition of oxidative stress with N-acetyl-L-cysteine (NAC) significantly restored SERCA expression in OIPN, indicating that oxidative stress downregulates SERCA2b in DRG. Collectively, these findings demonstrate that activation of SERCA2b by CDN1163 or *Schefflera kwangsiensis* extract enhances SERCA2b expression, reduces DRG neuronal sensitization, and alleviates OIPN. This work supports SERCA2b as a novel therapeutic target for OXA-induced neuropathy and expands the potential clinical analgesic indications of *Schefflera kwangsiensis*.

1. Introduction

Cancer represents a significant public health challenge and remains one of the leading causes of mortality worldwide. In 2024, an estimated 2.00 million new cancer cases and 0.61 million cancer-related deaths are projected to occur in the United States (US) [1]. Patients with cancer, like those with other chronic conditions, require sustained medical care, which imposes substantial financial burdens on healthcare systems and families. In the US, patients and caregivers incur monthly expenses of $180–2600, leading to increased out-of-pocket costs, medical debt, and potential bankruptcy [2]. Chemotherapy, particularly with platinum-based agents such as oxaliplatin (OXA), is effective in treating cancer but frequently causes adverse effects. OXA, used for advanced colorectal cancer, exhibits fewer hematological and gastrointestinal toxicities compared to other platinum compounds but induces neuropathic pain in approximately 95% of patients [3]. This neuropathy is characterized by sensory deficits and cold allodynia and is thought to be mediated, at least in part,

* Corresponding author.
E-mail addresses: zycao@cpu.edu.cn (Z. Cao); zhaofang0927@cpu.edu.cn (F. Zhao)
Δ These authors contributed equally to this work.

https://doi.org/10.1016/S1875-5364(26)61107-7

by oxalate, a major metabolite of OXA that aberrantly activates voltage-gated sodium channels (VGSCs) [4]. Platinum accumulation in the dorsal root ganglion (DRG) contributes to OXA-induced peripheral neuropathy (OIPN). Given the high prevalence and impact of this condition, novel therapeutic strategies are urgently needed, highlighting the importance of targeting the underlying mechanisms of OIPN.

The sarco/endoplasmic reticulum Ca^{2+}-ATPase (SERCA), a calcium transporter located in the endoplasmic reticulum (ER) membrane, plays a critical role in sequestering cytoplasmic Ca^{2+} into the ER lumen. Three SERCA isoforms are encoded by distinct genes: SERCA1 (predominantly expressed in fast-twitch skeletal muscle), SERCA2 (widely expressed, including in cardiac and sensory neurons), and SERCA3 (found in non-muscle tissues) [5]. Dysregulation of SERCA in DRG sensory neurons has been implicated in the pathogenesis of neuropathic pain. In models of nerve injury or diabetes, ER Ca^{2+} levels are reduced, particularly due to downregulation of SERCA2b, leading to neuronal hyperexcitability and ER stress [6, 7]. SERCA2b is the predominant SERCA isoform in rat DRG, and enhancing its activity, either through pharmacological activation with CDN1163 (CDN) or through overexpression, has been shown to relieve pain and restore neuronal function in chronic constriction injury (CCI) models by attenuating ER stress [8]. However, the specific role of SERCA2b in OIPN, and whether pharmacological activation of SERCA can alleviate OXA-induced neuropathic pain, has not yet been elucidated.

Schefflera kwangsiensis Merr. ex H.L. Li (SKM, *S. leucantha* R. Vig.) [9], a traditional Chinese medicinal herb native to Guangxi and Yunnan Provinces, has been used to treat pain, seizures, spasms, and stroke [10]. In China, several registered pharmaceutical products are derived from *Schefflera* species, including "Han Tao Ye Tablet" (Pharmacopoeia of the People's Republic of China, vol. 1, 2015 edition), which contains only *S. kwangsiensis* and is indicated for trigeminal neuralgia, sciatica, and rheumatic arthralgia. Phytochemical analyses have identified triterpenes, triterpenoid glycosides, and lupane saponins as major constituents [11], among which schekwanglupaside C has been identified as a potent SERCA activator [10].

This study investigated the role of SERCA2b in OIPN and evaluated its potential as a therapeutic target. We demonstrate that the SERCA activator CDN and an extract of *S. kwangsiensis* significantly alleviate OIPN in rats, with efficacy comparable to duloxetine (DLX). Activation of SERCA reduced voltage-gated sodium channel (VGSC)-associated neuronal hyperexcitability in DRG neurons, providing evidence that targeting SERCA activity may alleviate OIPN by normalizing sensory neuron excitability.

2. Materials and methods

2.1. Materials

OXA (CAS: 61825-94-3, Cat# O9512), DLX (CAS: 136434-34-9, Cat# Y0001454), CDN (CAS: 892711-75-0, Cat# SML1682), thapsigargin (TG, CAS: 67526-95-8, Cat# T9033), Hoechst 33342, 4-(2-hydroxyethyl)-1-piperazineethanesulfonic acid (HEPES), poly-D-lysine (CAS: 27964-99-4, Cat# P6407), nerve growth factor (NGF, CAS: 93928-24-6, Cat# N0513), N-acetyl-L-cysteine (NAC, CAS: 616-91-1, Cat# A7250), collagenase type I (CAS: 9001-12-1, Cat# C0130), and all inorganic chemicals were obtained from Sigma-Aldrich (St. Louis, MO, USA). Penicillin and streptomycin (Cat# 15070063), trypsin (Cat# 27250018), L-glutamine (200 mmol·L^{-1}, Cat# 25030081), fetal bovine serum (FBS, Cat# 10099141), Dulbecco's modified Eagle medium (DMEM, Cat# 11965092), and neurobasal medium (Cat# 21103049) were obtained from Life Technologies (Grand Island, NY, USA). Acetone (CAS: 67-64-1, Cat# 014106034) was purchased from Shanghai Titan Technology Co., Ltd. (Shanghai, China). SKM was purchased from Shaanxi Xintianyu Biotechnology Co., Ltd. (Xi'an, China). Antibodies against SERCA2 (Cat# 3183) and anti-mouse Alexa Fluor(R) 555 (Cat# 4409) were purchased from Cell Signaling Technology (Danvers, MA, USA). 2',7'-dichlorofluorescin diacetate (H_2DCFDA, Cat# HY-D0940, CAS: 4091-99-0) was purchased from MedChemExpress (Shanghai, USA). Annexin V-fluorescein isothiocyanate (FITC)/propidium iodide (PI) Apoptosis Detection Kit (Cat# 40302ES60) was purchased from Yeasen Biotechnology Co., Ltd. (Shanghai, China). Trizol reagent (Cat# R401), HiScript II Q RT SuperMix kit for quantitative polymerase chain reaction (qPCR) (Cat# R223), and SYBR qPCR Master Mix (Cat# Q331) were procured from Vazyme Biotech Co., Ltd. (Nanjing, China).

2.2. Animals

Animal experiments were conducted in accordance with the guidelines outlined in the National Institutes of Health Guide for the Care and Use of Laboratory Animals (NIH Publications No. 8023, revised 1978) and were approved by the China Pharmaceutical University Institutional Animal Care and Use Committee (#SYXK 2021-0011). The study design incorporated principles from the National Centre for the Replacement, Refinement, and Reduction of Animals in Research (NC3Rs), including randomization and blinded analysis, and ensured equal group sizes [12, 13]. Experiments followed the ARRIVE guidelines [12] and were powered based on prior experience to determine appropriate animal numbers and group sizes [14]. To minimize animal suffering and reduce the number of experimental animals, all necessary efforts were made. Male Sprague-Dawley rats (180–220 g) were obtained from Qing-Long-Shan Laboratory Animal Center (Nanjing, Jiangsu, China). The animals were housed in a temperature-controlled vivarium (23 ± 2 °C) under a 12-h light/dark cycle and provided food and water ad libitum.

2.3. Preparation of ethyl acetate extract of SKM (SKM.Ext)

The ethyl acetate-soluble fraction of SKM is enriched in lupane-type saponins [11]. Schekwanglupaside C, a lupane saponin isolated from *S. kwangsiensis*, has been reported to activate SERCA [10]. Briefly, 200 g of *S. kwangsiensis* powder (Shaanxi Xintianyu Biotechnology Co., Ltd.) was suspended in 1 L of H_2O and sequentially partitioned with petroleum ether (3 × 1 L) and ethyl acetate (3 × 1 L). The ethyl acetate layer was collected and concentrated under reduced pressure (−0.1 MPa, 55 °C) using a rotary evaporator. The resulting residue was further dried in a 55 °C oven until complete evaporation of the solvent. A total of 1.46 g of *S. kwangsiensis* ethyl acetate extract (SKM.Ext) was obtained and stored at 4 °C.

2.4. Ultra-high-performance liquid chromatography coupled with electrospray ionization quadrupole exactive orbitrap tandem mass spectrometry (UHPLC-ESI-QE-Orbitrap-MS) analysis

The chemical constituents of SKM were characterized by UHPLC–ESI–QE-Orbitrap-MS using a Vanquish UHPLC system and a Q Exactive Focus mass spectrometer (Thermo Fisher Scientific). The analysis was performed by BioTree (Shanghai, China) in accordance with published procedures [15]. Compound identification was based on mass spectral matching against the mzCloud, mzVault, and OTCML databases. Chromatographic separation was achieved on an ACQUITY UPLC BEH C18 column (2.1 mm × 100 mm, 1.7 μm). Putative active compounds were identified by matching MS and MS/MS spectra against the mzCloud, mzVault, and OTCML databases. Chromatographic separation was achieved on an ACQUITY UPLC BEH C18 column (2.1 mm × 100 mm, 1.7 μm). The mobile phase consisted of solvent A (0.1%

formic acid in water) and solvent B (0.1% formic acid in acetonitrile), with a flow rate of 0.5 mL·min^{-1} and an injection volume of 5 μL. The elution gradient was as follows: 0–11 min, 85% to 25% A; 11–12 min, 25% to 2% A; 12–14 min, held at 2% A; 14–14.1 min, 2% to 85% A; and 14.1–16 min, held at 85% A.

Both positive and negative ionization modes were employed. The mass spectrometer was operated with a scan range of *m/z* 100–1500, a spray voltage of 4.0 kV (positive mode) or −3.6 kV (negative mode), and a capillary temperature of 400 °C. Sheath gas and auxiliary gas flow rates were set to 45 and 15 Arb, respectively. Full-scan resolution was 70,000, and MS/MS scans were acquired at 17,500 resolution. Collision energies of 15, 30, and 45 were applied in NCE mode. Identified compounds were further validated by comparison with published literature.

2.5. Drug administration

CDN (repeated oral administration (p.o.), 2, 5, 10 mg·kg^{-1}), NAC (p.o., 100 mg·kg^{-1}), and SKM.Ext (p.o. 10, 20, 50 mg·kg^{-1}) were dissolved in a vehicle (Veh) solution containing 2% dimethyl sulfoxide (DMSO), 2% Tween-80 in saline, and 96% 0.5%-CMC-Na (0.5 g CMC-Na in 100 mL purified water). DLX (intraperitoneal (i.p.), 20 mg·kg^{-1}) was prepared in normal saline. For *in vitro* experiments, OXA (100 μmol·L^{-1}), TG (1 μmol·L^{-1}), CDN (3 μmol·L^{-1}), and SKM.Ext (1.5 μg·mL^{-1}) were dissolved in 0.1% DMSO. All drug administrations were performed under blinded conditions.

2.6. Induction of OIPN and drug administration

OIPN was induced as previously described [16]. Briefly, rats received intraperitoneal injections of OXA dissolved in 5% glucose (4 mg·kg^{-1}, i.p.) twice weekly on Days 1, 2, 8, 9, 15, and 16 to induce cold allodynia (acetone test) and mechanical allodynia (von Frey test). Control rats received equivalent volumes of vehicle (5% glucose, i.p.) on the same schedule. Behavioral assessments using the von Frey and acetone tests were performed before the first injection (Day 0) and at the indicated time points thereafter according to the experimental timeline.

2.7. Mechanical allodynia

Rats were placed on a wire mesh platform (20 cm × 15 cm × 20 cm, L × W × H) and allowed to acclimate for 15 min. Mechanical sensitivity was assessed using calibrated von Frey filaments applied perpendicularly to the plantar surface of the hind paw. A positive response was defined as a rapid withdrawal of the paw. The up-down method was used to determine the paw withdrawal threshold (PWT), continuing until a 50% withdrawal threshold was established.

2.8. Cold hyperalgesia

Cold hyperalgesia was evaluated using the acetone test as previously described [16]. Rats were placed in a transparent plastic chamber (20 cm × 15 cm × 20 cm, L × W × H) with a wire mesh floor and acclimated for 30 min. A total of 60 μL of acetone (Shanghai Titan Technology Co., Ltd., Shanghai, China) was applied to the plantar surface of each hind paw using an insulin needle (Penn Century Inc., Philadelphia, PA, USA), repeated three times per paw. The animals were observed for 40 s after each application, and the number of paw lifts or flinches was recorded. Each trial was repeated three times per side, resulting in six total trials. The cold pain score was assigned as follows: 0, no response; 1, quick withdrawal, flick, or stamping; 2, prolonged flicking; 3, repeated flicking with licking or biting of the hind paw [17].

2.9. Sample harvesting

Rats were anesthetized with sodium pentobarbital (1%, 40 mg·kg^{-1}, i.p.) and euthanized by CO_2 inhalation. L5 DRG tissues were carefully dissected and fixed in 4% paraformaldehyde for 24 h. After fixation, tissues were embedded in paraffin and sectioned at 4 μm thickness using a Leica RM2255 automated microtome (Leica Instruments GmbH, Nussloch, Germany) for subsequent hematoxylin-eosin (H&E) staining and immunofluorescence analysis. L4 and L6 DRG tissues were collected separately for ribonucleic acid (RNA) extraction and qPCR analysis [18].

2.10. H&E staining of DRG

Stained tissue sections were imaged using a digital color camera mounted on an inverted microscope (Nikon, Tokyo, Japan), with image acquisition controlled by NIS-Elements BR software (Version 4.30.01, Nikon).

2.11. Immunofluorescence of DRG

Deparaffinized and antigen-retrieved sections were blocked with 5% bovine serum albumin (BSA) for 30 min and incubated overnight at 4 °C with anti-SERCA2 antibody (1∶300). After washing with PBS, sections were incubated for 1 h at room temperature with Alexa Fluor 555-conjugated goat anti-mouse secondary antibody (1∶1000). Nuclei were counterstained with Hoechst 33342 (10 μg·mL^{-1}) for 10 min. Fluorescence images were captured from randomly selected fields using a fluorescence microscope (DMI 8, Leica Microsystems GmbH, Wetzlar, Germany).

2.12. Real-time quantitative reverse transcription-PCR (RT-PCR) analysis

Messenger RNA (mRNA) expression levels were quantified using the $2^{-\Delta\Delta Ct}$ method, with GAPDH used as the internal reference gene. Primer sequences are listed in Supplemental Table 1.

2.13. Primary cultures of DRG neurons

DRG were dissected from newborn Sprague-Dawley rats and digested at 37 °C for 25 min in DMEM-F12 containing 0.5 mg·mL^{-1} trypsin and 1 mg·mL^{-1} collagenase type I. After centrifugation (100 *g*, 3 min), the tissue pellet was resuspended in DMEM-F12 supplemented with 10% FBS, 1% GlutaMAX, 1% penicillin/streptomycin, 1% HEPES, and 50 ng·mL^{-1} NGF. Cells were plated at a density of 1,000 cells per 35-mm dish pre-coated with poly-D-lysine (10 μg·mL^{-1}) and maintained in a humidified incubator with 5% CO_2 for patch-clamp and current-clamp recordings after a 2-h attachment period.

2.14. Whole-cell current-clamp recordings

Action potentials in small- and medium-sized DRG neurons (diameter < 35 μm) from newborn rats were recorded using current-clamp techniques with an EPC-10 amplifier (HEKA Electronics, Germany), as previously described [19]. Patch pipettes were pulled from 1.5 mm capillary glass to a resistance of 3–4 MΩ and filled with intracellular solution (in mmol·L^{-1}: KCl 140, $MgCl_2$ 5, $CaCl_2$ 2.5, EGTA 5, HEPES 5, Mg-ATP 3; pH adjusted to 7.2 with KOH), yielding final pipette resistances between 2.0 and 5.0 MΩ. The extracellular solution contained (in mmol·L^{-1}) NaCl 135, KCl 4.7, $MgCl_2$ 1, $CaCl_2$ 1, HEPES 10, glucose 10; pH 7.4 adjusted with NaOH. Liquid junction potentials were corrected. Rheobase was determined by applying 1000-ms current injections from 20 to 280 pA in 20-pA increments. To assess changes in firing frequency induced by Veh, OXA, TG, CDN, or SKM.Ext, a 100 pA cur-

rent was applied for 1000 ms, and the number of action potentials within 1 s was recorded.

2.15. Whole-cell patch-clamp recordings

The extracellular solution contained (in mmol·L^{-1}): NaCl 30, $MgCl_2$ 1, KCl 5, $CaCl_2$ 1.8, CsCl 5, D-glucose 25, TEA-Cl 90, HEPES 5; pH adjusted to 7.4 with NaOH. The intracellular solution consisted of (in mmol·L^{-1}): CsF 135, NaCl 10, HEPES 5; pH adjusted to 7.3 with CsOH. To examine the effects of OXA, CDN, and SKM.Ext on voltage-dependent Na^+ currents, depolarizing voltage steps were applied as previously described [14].

2.16. Assessment of reactive oxygen species (ROS) levels

Intracellular ROS levels were measured using the fluorescent probe H_2DCFDA, as previously described [8]. Primary DRG neurons were pre-treated with Veh, 3 μmol·L^{-1} CDN, or 1.5 μg·mL^{-1} SKM.Ext for 1 h, followed by 12 h of exposure to Veh or 100 μmol·L^{-1} OXA. Cells were then incubated with 5 μmol·L^{-1} H_2DCFDA at 37 °C for 30 min. Fluorescence was visualized using a confocal laser scanning microscope (LSM800, Zeiss, Oberkochen, Germany) with excitation at 488 nm and emission detection at 525 nm.

2.17. Annexin V-FITC/PI apoptosis/necrosis assay

Primary DRG neurons were pre-incubated with Veh, 3 μmol·L^{-1} CDN, or 1.5 μg·mL^{-1} SKM.Ext for 1 h, followed by 12 h of treatment with Veh or 100 μmol·L^{-1} OXA. Cells were then stained with a solution containing 1 × Binding Buffer, Annexin V-FITC, and PI in a 200∶1∶2 ratio and incubated in the dark for 15 min. Fluorescence images were captured from random fields using a DMI 8 fluorescence microscope (Leica Microsystems GmbH, Wetzlar, Germany). The percentage of apoptotic/necrotic neurons was calculated as (Annexin V-FITC$^+$/PI$^+$) × 100% divided by the number of round cells (10–50 μm in diameter) in bright-field images. Late apoptotic and necrotic cells were identified by dual positivity for Annexin V-FITC and PI (Yeasen, Cat# 40302ES60) [20,21].

2.18. Statistical analysis

Group size corresponded to the number of independent biological replicates (one data point per rat, tissue section, or neuron), with technical replicates not considered independent. Statistical analyses were performed only when group size was at least n = 4. Current-clamp data were acquired using Patchmaster (HEKA Electronics, 2016) and analyzed with OriginPro (Version 8, OriginLab, Northampton, MA, USA). Immunofluorescence signal intensities were normalized to the Veh group. All summary data are presented as mean ± SEM and analyzed using GraphPad Prism (Version 8.0, GraphPad Software Inc., San Diego, CA, USA). Statistical significance was evaluated using Student's t-test or one-way analysis of variance (ANOVA) (ordinary or repeated measures). When ANOVA yielded a significant F value (P < 0.05), a post hoc Bonferroni test was applied. A P value < 0.05 was considered statistically significant. All datasets were tested for normality and homogeneity of variance.

3. Results

3.1. L4–L6 DRG neurons from OIPN rats exhibit reduced expression of SERCA2b

OXA (i.p. in 5% glucose at a dose of 4 mg·kg^{-1}, administered twice weekly on days 1, 2, 8, 9, 15, and 16) induced cold allodynia and mechanical allodynia in male rats, as assessed on days 0, 7, 14, and 21 (Fig. 1A). This was evidenced by a time-dependent decrease in paw withdrawal threshold (Fig. 1B) and an increased acetone response score (Fig. 1C). H&E staining revealed that L5 DRG neurons from Veh-treated rats (5% glucose) exhibited normal morphology, with well-defined cellular boundaries, intact nucleoli, and a clear cytoplasmic outline (Fig. 1D, upper panel). In contrast, OXA-treated rats displayed signs of neuronal cell body shrinkage (Fig. 1D, lower panel). The mean diameter of L5 DRG neurons was significantly reduced in OXA-treated rats compared to Veh-treated controls, suggesting selective loss, immune-mediated destruction, or apoptosis of large-diameter neurons (Fig. 1E). In the DRG, pro-inflammatory cytokines including tumor necrosis factor α (TNF-α), interleukin-1β (IL-1β), and IL-6 contribute significantly to neuropathic pain by amplifying nociceptive signaling and sensitizing ion channels; mRNA levels of these cytokines were significantly elevated in OXA-treated rats (Fig. 1F). Immunofluorescence staining demonstrated a significant reduction in SERCA2b protein expression in the L5 DRG of rats with OXA-induced neuropathic pain (Figs. 1G & 1H left panel). Consistent with decreased protein levels, *Serca2b* mRNA expression in the L4 and L6 DRG was significantly downregulated in OXA-treated rats by day 22 (Fig. 1H right panel). Collect-

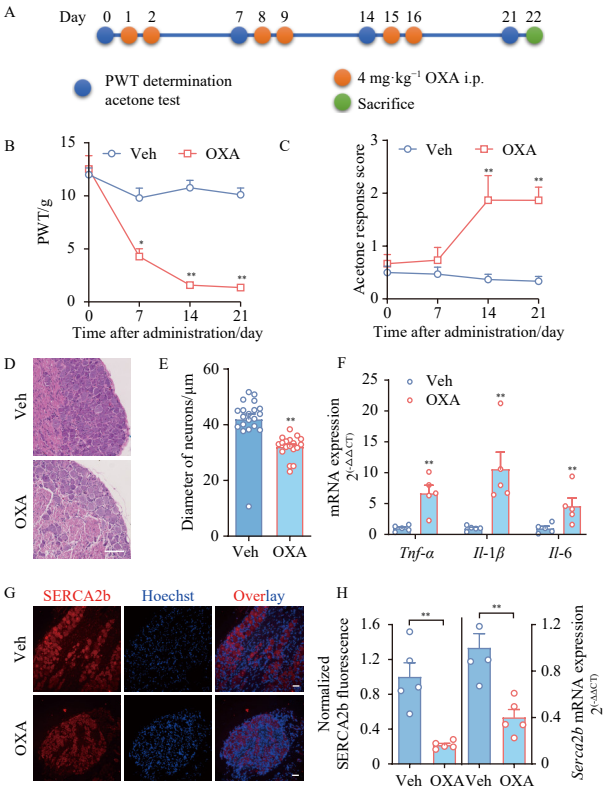

Fig. 1 L4–L6 DRGs from OIPN rats showed decreased mRNA and protein levels of SERCA2b. (A) Experimental timeline for OIPN induction and behavioral testing. (B) Paw withdrawal mechanical threshold (PWT) before and after OXA or vehicle (Veh) administration on the indicated days. (C) Acetone test scores before and after OXA or Veh administration on the indicated days. n = 6. $^*P$ < 0.05 *vs.* Veh group, $^{**}P$ < 0.01 *vs* Veh group. (D) Representative H&E-stained images of L5 DRG from vehicle (Veh)-treated and OXA-treated rats on Day 22. Scale bar = 100 μm. (E) DRG sensory neurons, characterized by large central nuclei with prominent nucleoli and abundant cytoplasm, were analyzed for somatic diameter in L5 DRG from Veh and OXA groups. n = 20. $^{**}P$ < 0.01 *vs* Veh group. (F) Quantitative RT-PCR analysis of *tnf-α*, *il-1β*, *il-6* mRNA levels in L4 and L6 DRG of rats. n = 5. $^{**}P$ < 0.01, *vs* Veh group. (G) Representative immunofluorescent images of Hoechst 33342 (blue) and SERCA2b (red) labeled L5 DRG from Veh and OIPN rats. Scale bar = 50 μm. (H) Left: Quantification of SERCA2b immunofluorescence intensity in L5 DRG of Veh and OIPN rats. n = 5. $^{**}P$ < 0.01. Right: quantitative RT-PCR analysis of *Serca2b* mRNA levels in L4 and L6 DRG of rats. n = 4–5. $^{**}P$ < 0.01 *vs* Veh group. Student's t-test. Data are presented as Mean ± SEM.

ively, these findings indicate that downregulation of SERCA2b in DRG neurons plays a regulatory role in the pathogenesis of OIPN.

3.2. Increasing SERCA activity reduces mechanical and cold allodynia, enhancing SERCA2b overexpression, and relieves DRG neuron shrinkage in rats with OIPN

CDN1163 is a small-molecule SERCA activator that elevates ER Ca^{2+} levels and protects neurons from ER stress-induced apoptosis *in vitro* [22]. In our OIPN model, OXA administration induced both cold and mechanical allodynia in male rats, as evidenced by decreased PWTs and increased acetone response scores (Figs. 2A–2C). The sustained effect of SERCA activation was assessed by repeated oral dosing of CDN1163 (2, 5, and 10 mg·kg^{-1}) and intraperitoneal DLX (20 mg·kg^{-1}) from day 10 to day 19 (Fig. 2A). To compare treatment efficacy, we calculated the area under the curve (AUC) for PWT and acetone response scores from days 16 to 21. OXA-treated rats developed significant mechanical allodynia, reflected by lower PWT relative to vehicle controls, whereas oral CDN1163 and intraperitoneal DLX significantly increased PWT in OXA-treated rats (Fig. 2D). Similarly, OXA induced marked cold allodynia, with elevated acetone response scores, which were significantly attenuated by CDN1163 and DLX (Fig. 2E). Collectively, these findings indicate that pharmacological enhancement of SERCA activity by CDN1163 reduces both mechanical and cold allodynia in rats with OIPN.

H&E staining of the L5 DRG on day 22 following OIPN induction revealed that 14 days of repeated oral administration of CDN reduced the severity of neuronal damage (Figs. 2F & 2H). The diameter of DRG neurons was significantly reduced in OXA-treated

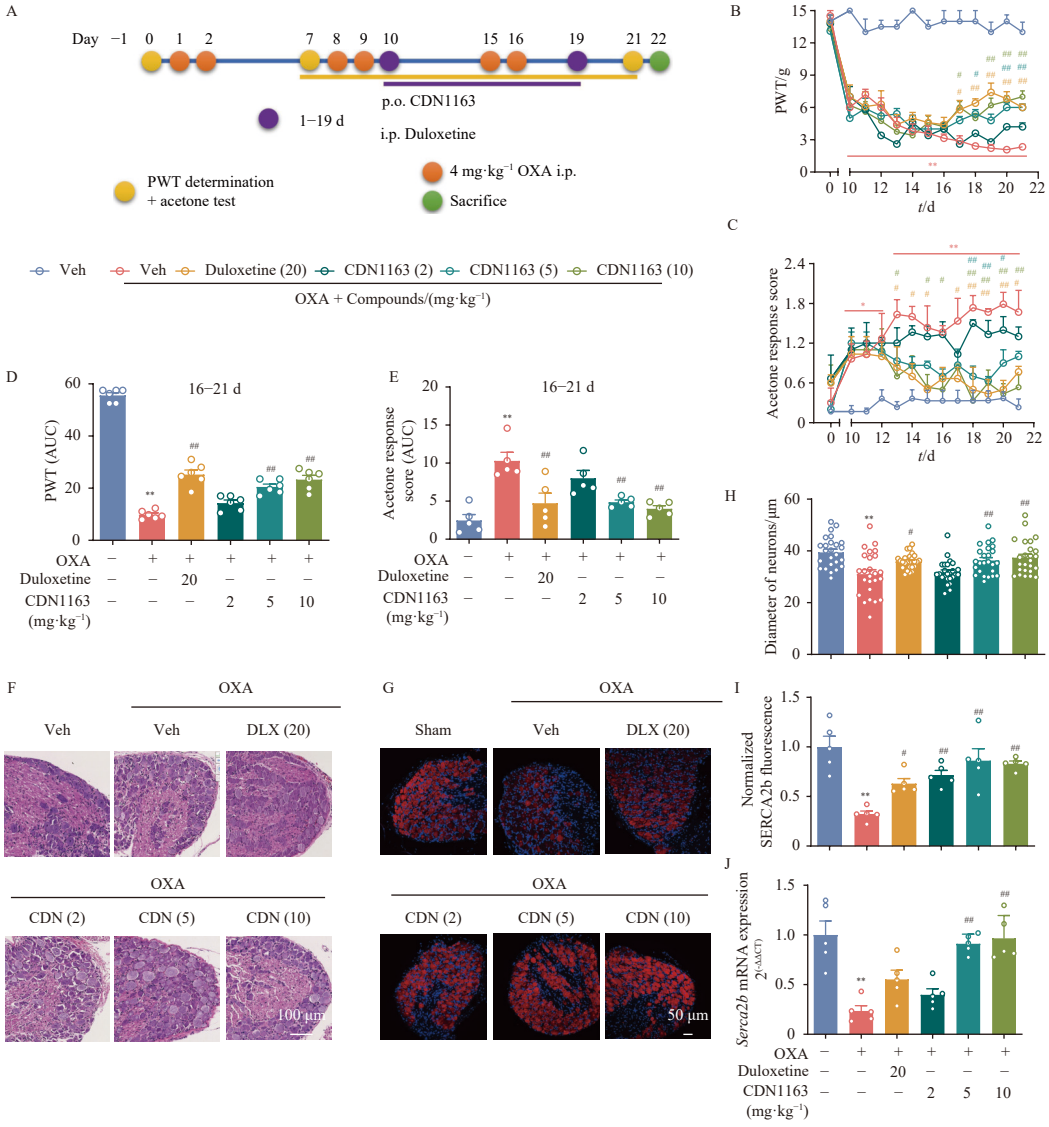

Fig. 2 Repeated oral administration of CDN1163 produced progressive and long-lasting alleviation of OIPN, alleviated the shrinkage of DRG neurons and increased mRNA and protein expression levels of SERCA2b in OIPN rats. (A) A schematic illustrating the schedule for drug administration, tissue collection, and behavioral assessments. Starting on day 10 of OIPN, Veh or varying doses of CDN1163 (CDN) were given orally (p.o.) once daily for 10 consecutive days, while DLX was administered intraperitoneally (i.p.) once daily for 10 consecutive days after PWT determination and acetone teat, to avoid detecting the acute analgesic effects of CDN and DLX. PWT and acetone response scores were measured on days 0, 7–21, with L4– L6 DRG collected on day 22. The effect of repeated administration of CDN1163 and DLX on mechanical (B) and cold allodynia (C) post-OIPN is shown. Data were analyzed using two-way ANOVA with tukey 's multiple comparisons test. $^{*}P < 0.05$, $^{**}P < 0.01$ *vs* Veh group. $^{\#}P < 0.05$, $^{\#\#}P < 0.01$ *vs* OXA group. (D) A bar graph depicting the area under the curve (AUC) of PWT from days 16 to 21 for both p.o. CDN1163 and i.p. DLX, $n = 6$. (E) Another bar graph showing the AUC for acetone response score in the same timeframe for p.o. CDN1163 and i.p. DLX, $n = 5$. (F) Representative H&E-stained photomicrographs of L5 DRG in OIPN rats treated with oral CDN1163 at doses of 2, 5, and 10 mg·kg^{-1}, or intraperitoneal DLX at 20 mg·kg^{-1}. Scale bar = 100 μm. (G) Representative immunofluorescent images of Hoechst 33342 (blue) and SERCA2b (red) in L5 DRG of Veh and OIPN rats. Scale bar = 50 μm. (H) Measurement of L5 DRG neuron diameters in OIPN rats following p.o. CDN1163 (2, 5, 10 mg·kg^{-1}) or i.p. DLX (20 mg·kg^{-1}). $^{**}P < 0.01$ *vs* Veh group. $^{\#\#}P < 0.05$, $^{\#\#}P < 0.01$ *vs* OXA group, $n = 25$. (I) Quantification of SERCA2b immunofluorescence intensity in L5 DRG of Veh and OIPN rats. $n = 5$. (J) Quantitative RT-PCR analysis of *Serca2b* mRNA levels in the L4–6 DRG of rats, $n = 5$. $^{**}P < 0.01$ *vs* Veh group. $^{\#}P < 0.05$, $^{\#\#}P < 0.01$ *vs* OXA group. Data were analyzed using one-way ANOVA with Bonferroni's multiple comparisons test. Results are expressed as Mean ± SEM.

rats, but both CDN and DLX treatment restored neuronal diameter, with CDN showing a dose-dependent effect (Figs. 2F & 2H). In addition, in DRG from OXA-treated rats, repeated CDN1163 administration fully restored SERCA2b protein expression (Figs. 2G & 2I) and mRNA expression (Fig. 2J) to values comparable to those of vehicle-treated controls.

3.3. CDN1163 reduces DRG inflammation in OIPN rats and alleviates hyperexcitability by decreasing the window current of VGSCs in DRG neurons.

Quantitative RT-PCR analysis showed that mRNA expression levels of *Tnf-α* and *Il-1β* were significantly elevated in L4 and L6 DRG tissues of OIPN rats. Treatment with CDN and DLX markedly reduced the expression of *Tnf-α* and *Il-1β* in the DRG, with CDN exhibiting a dose-dependent effect (Figs. 3A & 3B). Previous studies have indicated that OXA incubation enhances VGSC currents and increases VGSC density [23], contributing to neuronal hyperexcitability and pain hypersensitivity. Exposure to 100 μmol·L^{-1} OXA for 24 h increased VGSC current density in primary cultured DRG neurons (Fig. 3C). The peak current density was elevated following OXA treatment, but this increase was inhibited by 1-h preincubation with 3 μmol·L^{-1} CDN (Fig. 3C). The window current refers to a small persistent Na^+ current that occurs within a specific voltage range where the steady-state activation and inactivation curves of VGSCs overlap, indicating a mixed open/inactivated state of the channels [24]. This overlap allows a fraction of Na^+ channels to remain open at resting membrane potentials, contributing to spontaneous depolarization (Fig. 3D). CDN reduced the abnormal increase in window current induced by OXA in DRG neurons (Fig. 3D). Consistent with prior reports [8, 25], both OXA exposure and SERCA inhibition with TG reduced rheobase and increased firing frequency in DRG neurons, leading to hyperexcitability (Figs. 3E–3G). CDN (3 μmol·L^{-1}) alone had no significant effect on rheobase or firing frequency (Figs. 3H, 3J, & 3K). However, pre-incubation with 3 μmol·L^{-1} CDN for 1 h reversed OXA-induced hyperexcitability in L4–L6 DRG neurons (Figs. 3I–3K). The action potential rheobase was significantly lower in OXA- and TG-treated neurons compared to Veh-treated neurons (Fig. 3J). Firing frequency in L4–L6 DRG neurons was significantly increased in OXA- and TG-treated groups but was substantially reduced by pre-incubation with CDN (Fig. 3K). In summary, CDN may reduce OXA-induced neuronal hyperexcitability *in vitro* by suppressing VGSC current density and window current.

3.4. Inhibiting OXA-induced oxidative stress in DRG can significantly improve SERCA2b downregulation

OXA-induced ROS production and pro-inflammatory cytokines contribute to ER stress [26]. Given that reduced SERCA activity leads to the accumulation of unfolded proteins and ER stress in pancreatic β-cells [27], we investigated whether oral administration of the antioxidant NAC could enhance SERCA2b expression in the DRG under OIPN conditions, thereby mitigating neuroinflammation. To evaluate the long-term effects of antioxidant treatment, repeated oral doses of NAC (100 mg·kg^{-1}) were administered from day 1 to day 21 (Fig. S1A). NAC treatment gradually improved PWT and reduced acetone response scores (Fig. S1B). H&E staining of the L5 DRG on day 22 post-OIPN showed that 21 days of repeated oral NAC administration reduced the

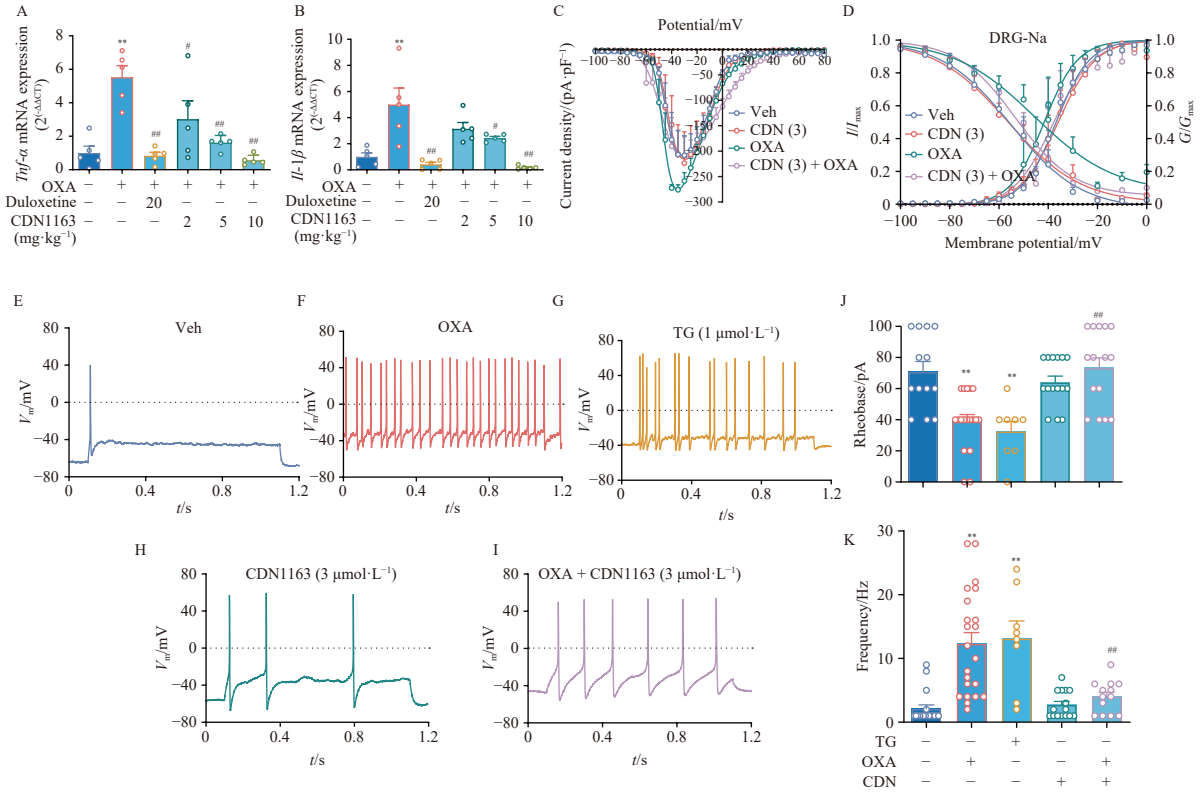

Fig. 3 CDN1163 suppressed the OXA-induced neuroinflammation in DRG of OIPN rats, reduced sodium current density, and significantly mitigated OXA-induced hypersensitivity in DRG neurons. Quantitative RT-PCR analysis of (A) *tnf-α* and (B) *il-1β* mRNA levels in the L4 and L6 DRG of rats, $n = 5$. (C) Current-voltage (I-V) relationships of VGSCs in the Veh, 100 μmol·L^{-1} OXA treated 24 h, 3 μmol·L^{-1} CDN1163 treated 25 h, preincubated with 3 μmol·L^{-1} CDN1163 for 1 h followed by 100 μmol·L^{-1} OXA treatment for 24 h DRG neurons. (D) Steady-state activation and inactivation curves of VGSC in the Veh, 100 μmol·L^{-1} OXA treated 24 h, 3 μmol·L^{-1} CDN1163 treated 25 h, preincubated with 3 μmol·L^{-1} CDN1163 for 1 h followed by 100 μmol·L^{-1} OXA treatment for 24 h DRG neurons. Representative action potential firing induced by a 100-pA current injection in multiple spiking firing DRG neurons from (E) Veh and (F) 100 μmol·L^{-1} OXA treated 24 h, (G) 1 μmol·L^{-1} TG treated 24 h, (H) 3 μmol·L^{-1} CDN1163 treated 25 h, (I) neurons preincubated with 3 μmol·L^{-1} CDN1163 for 1 h followed by 100 μmol·L^{-1} OXA treatment for 24 h. (J) Rheobase quantification is required to evoke action potentials in DRG neurons from Veh, OXA, and TG-treated groups, with or without CDN1163. $n = 8–15$. $^{**}P < 0.01$ *vs* Veh. $^{\#\#}P < 0.01$ *vs* OXA. (K) Quantification of firing frequency in DRG neurons from Veh, OXA, TG treated DRG neurons with or without CDN1163. $n = 15–25$. $^{**}P < 0.01$ *vs* Veh. $^{\#\#}P < 0.01$ *vs* OXA. Data were analyzed using one-way ANOVA followed by Bonferroni's multiple comparisons test, with results shown as Mean ± SEM.

severity of neuronal damage (Fig. S1C). In the OXA-treated group, NAC administration significantly reduced the elevated mRNA levels of *Tnf-α*, *Il-1β*, and *Il-6* compared to OXA alone (Fig. S1D). Furthermore, repeated p.o. administration of NAC increased both SERCA2b protein and mRNA expression in the DRG of OXA-treated rats (Fig. S1E). These data indicate that NAC alleviates mechanical and cold allodynia in OIPN rats, potentially through upregulation of *Serca2b* expression in the DRG.

3.5. Chemical profiling of SKM.Ext and its effects on mechanical and cold allodynia in rats with OIPN

SKM (Araliaceae) is rich in lupane-type saponins with known SERCA-activating properties [10, 11]. In this study, the chemical constituents of SKM were identified using UHPLC-ESI-QE-Orbitrap-MS analysis. According to the 2020 edition of the Chinese Pharmacopoeia, rutin is the standardized marker compound for Hantao Ye (Fig. 4A, compound **9**). Additionally, fumaric acid has been proposed as another potential marker compound for Hantao Ye (Fig. 4B, compound **4**). The molecular formulas, measured *m/z*, calculated *m/z*, and corresponding literature sources for 14 identified components in SKM are listed in Table 1. Due to the technical challenges in isolating and characterizing structurally complex compounds such as schekwanglupaside A ($C_{44}H_{70}O_{14}$), schekwanglupaside B ($C_{43}H_{68}O_{13}$) [11], and schekwanglupaside C ($C_{64}H_{104}O_{27}$) [10], these were not included in Figs. 4A & 4B and Table 1.

Repeated oral administration of SKM.Ext (10, 20, and 50 mg·kg^{-1}) and intraperitoneal administration of DLX (20 mg·kg^{-1}) was performed from day 10 to day 19 (Fig. 4C). Both DLX and SKM.Ext gradually increased PWT and reduced acetone response scores in a dose-dependent manner, with effects persisting until at least day 21, two days after treatment cessation (Figs. 4D & 4E). The AUC of PWT was significantly lower in OXA-treated rats than in Veh-treated rats, but both oral administration of SKM.Ext and intraperitoneal administration of DLX significantly increased PWT, thereby alleviating mechanical allodynia (Fig. 4F). Similarly, the AUC of the acetone response score was significantly higher in OXA-treated rats, but both SKM.Ext and DLX significantly reduced this score, indicating alleviation of cold allodynia (Fig. 4G).

3.6. SKM.Ext upregulates the expression of SERCA2b in the DRG, alleviating neuronal shrinkage and inflammation in the DRG of OIPN rats

SKM.Ext treatment in OXA-treated rats restored *Serca2b*

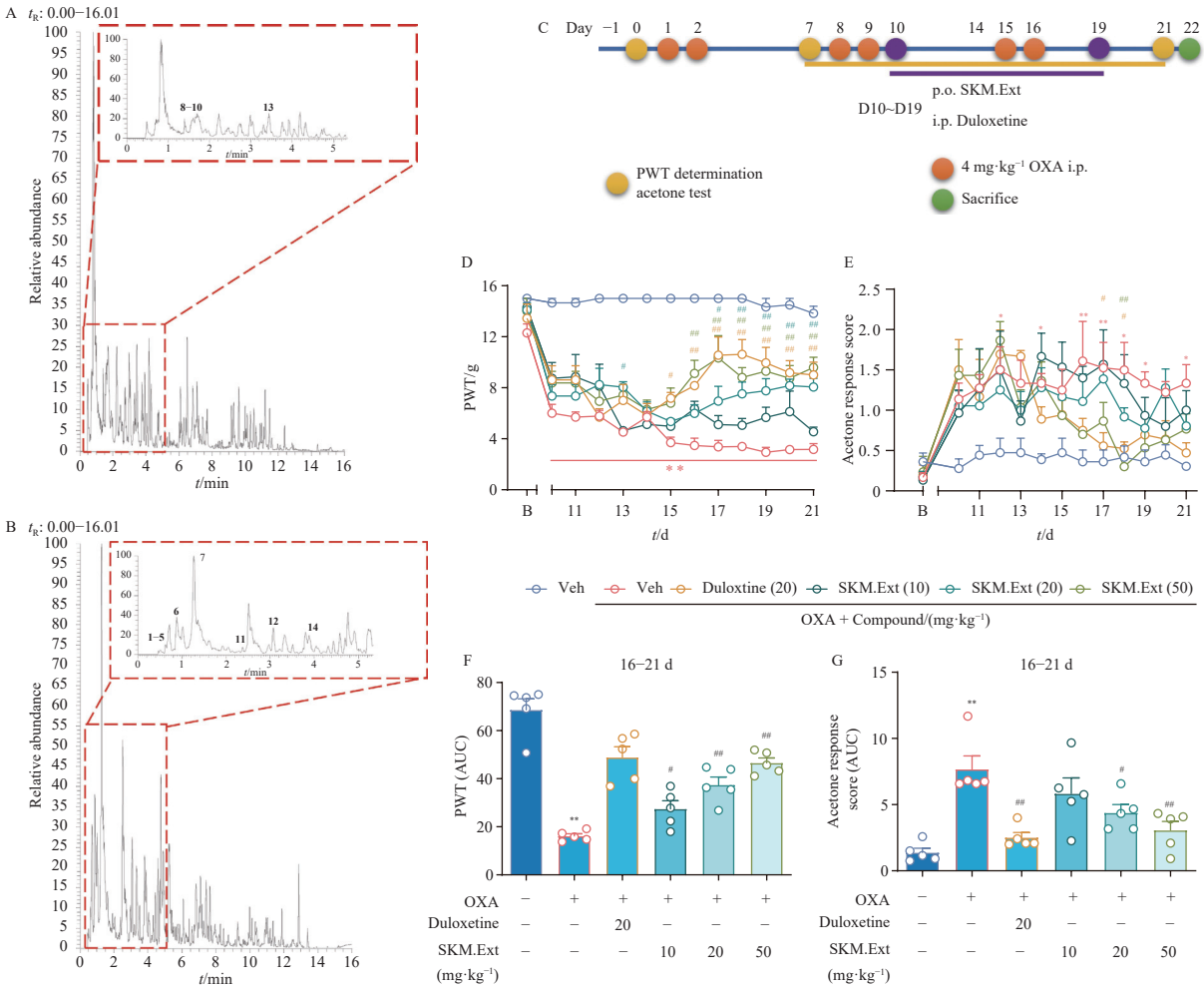

Fig. 4 Total ion chromatograms of constituents in SKM.Ext and its sustained analgesic effects in OIPN rats. (A) Total ion chromatogram of SKM.Ext in positive ion mode. (B) Total ion chromatogram of SKM.Ext in negative ion mode. (C) Experimental timeline for drug administration, behavioral testing, and tissue collection. From day 10 after OIPN induction, Veh or SKM.Ext (10, 20, 50 mg·kg^{-1}) was administered once daily for 10 consecutive days, and DLX was administered intraperitoneally (i.p.) once daily for 10 consecutive days. Behavioral tests were always performed before daily dosing to avoid confounding by acute analgesic effects of SKM.Ext or duloxetine. Paw withdrawal threshold (PWT) and acetone response scores were recorded on days 0 and 7–21, and L4–L6 DRGs were collected on day 22. Effect of repeated SKM.Ext and duloxetine administration on (D) mechanical allodynia and (E) cold allodynia in OIPN rats, $n = 5$. Data were analyzed using two-way ANOVA followed by Tukey's multiple comparisons test. $^{*}P < 0.05$, $^{**}P < 0.01$, *vs* Veh group. $^{\#}P < 0.05$, $^{\#\#}P < 0.01$, *vs* OXA group. (F) Area under the curve (AUC) for PWT from days 16–21 in Veh, SKM.Ext, and duloxetine groups, $n = 5$. (G) AUC for acetone response scores from days 16–21 in the same treatment groups, $n = 5$. Data were analyzed using one-way ANOVA with Bonferroni's multiple comparisons test. Results are expressed as Mean ± SEM.

Table 1 The detected ion chromatogram of constituents in SKM.

No.	t_R/(min)	m/z		Ion mode	ppm	Identification	Formula	Reference
		Measured	Calculated					
1	0.208 68	137.024 22	137.024 42	[M − H]⁻	−1.459 594	4-Hydroxybenzoic acid	$C_7H_6O_3$	61
2	0.520 12	133.014 21	133.014 25	[M − H]⁻	−0.300 720	Malic acid	$C_4H_6O_5$	62
3	0.564 58	117.019 29	117.019 33	[M − H]⁻	−0.341 824	Succinic acid	$C_4H_6O_4$	62
4	0.615 18	115.003 81	115.003 68	[M − H]⁻	1.130 399	Fumaric acid	$C_4H_4O_4$	63
5	0.673 61	299.113 18	299.113 63	[M − H]⁻	−1.504 445	Rhodioloside	$C_{14}H_{20}O_7$	64
6	0.913 99	179.034 70	179.034 98	[M − H]⁻	−1.563 940	Caffeic acid	$C_9H_8O_4$	61
7	1.276 64	121.029 45	121.029 50	[M − H]⁻	−0.413 122	4-Hydroxy-benzaldehyde	$C_7H_6O_2$	61
8	1.392 10	303.049 67	303.049 93	[M + H]⁺	−0.857 944	Quercetin	$C_{15}H_{10}O_7$	65
9	1.449 99	611.161 12	611.160 66	[M + H]⁺	0.752 666	Rutin	$C_{27}H_{30}O_{16}$	66
10	1.519 41	153.054 76	153.054 62	[M + H]⁺	0.914 706	Vanillin	$C_8H_8O_3$	67
11	2.393 00	417.154 19	417.155 49	[M − H]⁻	−3.116 344	(+)-Syringaresinol	$C_{22}H_{26}O_8$	67
12	3.195 85	207.066 07	207.066 28	[M − H]⁻	−1.014 168	Sinapaldehyde	$C_{11}H_{12}O_4$	67
13	3.447 57	179.070 34	179.070 27	[M + H]⁺	0.390 908	Coniferaldehyde	$C_{10}H_{10}O_3$	67
14	4.001 33	271.060 96	271.061 20	[M − H]⁻	−0.885 409	Naringenin	$C_{15}H_{12}O_5$	68

mRNA expression to levels similar to those in Veh-treated controls, with a significant increase compared to OXA alone (Fig. 5A). H&E staining of the L5 DRG on day 22 post-OIPN demonstrated that repeated oral administration of SKM.Ext reduced the extent of neuronal damage (Fig. 5B). The diameter of DRG neurons was reduced in OXA-treated rats, but both SKM.Ext and DLX treatments significantly restored neuronal diameter (Fig. 5C). OXA treatment significantly increased mRNA levels of *Tnf-α*, *Il-1β*, and *Il-6*, while oral administration of SKM.Ext (10, 20, 50 mg·kg^{-1}) and intraperitoneal administration of DLX (20 mg·kg^{-1}) significantly reduced their expression in the DRG (Fig. 5D). These results indicate that SKM.Ext mitigates neuronal shrinkage and inflammation in the DRG by enhancing SERCA2b expression, thereby alleviating mechanical and cold allodynia in OIPN rats.

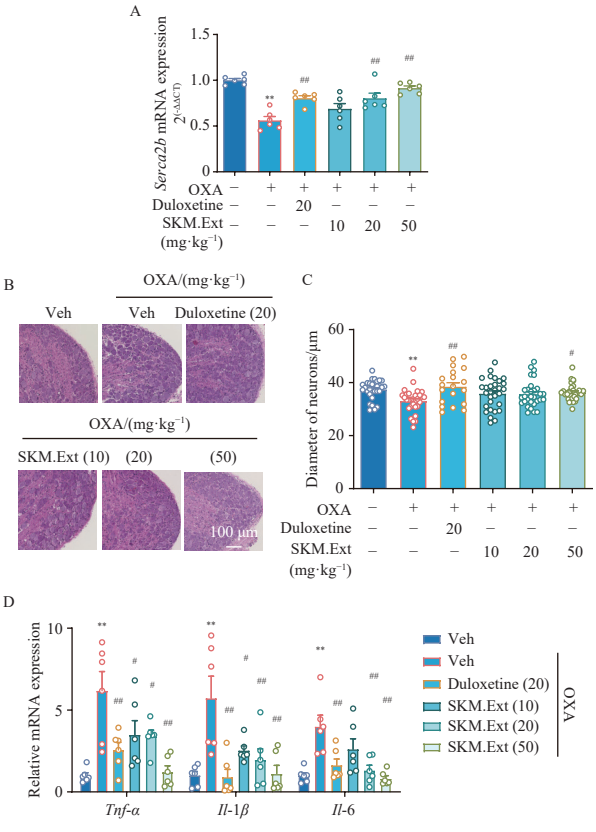

Fig. 5 Repeated oral administration of SKM.Ext increased *Serca2b* mRNA, alleviated the shrinkage of DRG neurons, and reduced neuroinflammation in OIPN rats. (A) Quantitative RT-PCR analysis of *Serca2b* mRNA levels in the L4 and L6 DRG of rats. n = 6. (B) Representative H&E-stained photomicrographs of L5 DRG in OIPN rats treated with oral SKM.Ext at doses of 10, 20, and 50 mg·kg^{-1}, or intraperitoneal DLX at 20 mg·kg^{-1}. Scale bar = 100 μm. (C) Measurement of L5 DRG neuron diameters in OIPN rats following p.o. SKM.Ext (10, 20, 50 mg·kg^{-1}) or i.p. DLX (20 mg·kg^{-1}). n = 19–30. $^{**}P < 0.01$ *vs* Veh group. $^{\#}P < 0.05$, $^{\#\#}P < 0.01$ *vs* OXA group. (D) Quantitative RT-PCR analysis of *tnf-α*, *il-1β* and *il-6* mRNA levels in the L4 and L6 DRG of rats. n = 6. $^{**}P < 0.01$ *vs* Veh group. $^{\#\#}P < 0.01$ *vs* OXA group. Data were analyzed using one-way ANOVA followed by Bonferroni's multiple comparisons test and expressed as Mean ± SEM.

3.7. SKM.Ext alleviates the OXA-induced hyperexcitability in DRG neurons

Consistent with the findings in Fig. 3, 24-h pre-incubation with 100 μmol·L^{-1} OXA significantly increased VGSC current density (Figs. 6A & 6B), induced membrane depolarization, and reduced rheobase, leading to increased neuronal excitability (Figs. 6C, 6D, 6G & 6H). Pre-incubation with 1.5 μg·mL^{-1} SKM.Ext for 1 h effectively inhibited the OXA-induced increase in current density and window current after 24 h (Figs. 6A & 6B). Moreover, SKM.Ext pre-treatment significantly reversed the OXA-induced reduction in rheobase and the increase in firing frequency in DRG neurons (Fig. 6C–6H). In summary, similar to the SERCA activator CDN, SKM.Ext may reduce OXA-induced neuronal hyperexcitability *in vitro* by suppressing VGSC current density.

3.8. Activation of SERCA significantly alleviates OXA-induced oxidative stress and apoptosis/necrosis in the DRG

OXA exerts its anti-tumor effects primarily by inducing DNA damage and increasing ROS production, ultimately triggering apoptosis and necrosis [28]. Since Hoechst nuclear staining cannot distinguish satellite glial cells [29], DRG neurons were identified as round cells with diameters ranging from 10 to 50 μm under bright-field microscopy. Based on this, we investigated whether SERCA activators, CDN and SKM.Ext, could attenuate OXA-induced ROS accumulation and thereby reduce apoptosis and necrosis in DRG neurons. Both 3 μmol·L^{-1} CDN and 1.5 μg·mL^{-1} SKM.Ext mitigated oxidative stress induced by 100 μmol·L^{-1} OXA after 12 h of exposure (Figs. 7A & 7B). Additionally, both compounds reduced OXA-induced apoptosis and necrosis in DRG neurons after 12 h (Figs. 7C & 7D).

4. Discussion

The attachment of platinum to mitochondrial DNA disrupts its normal functions, impairing replication and transcription. These impairments compromise the mitochondrial respiratory chain and elevate oxidative stress, ultimately causing peripheral

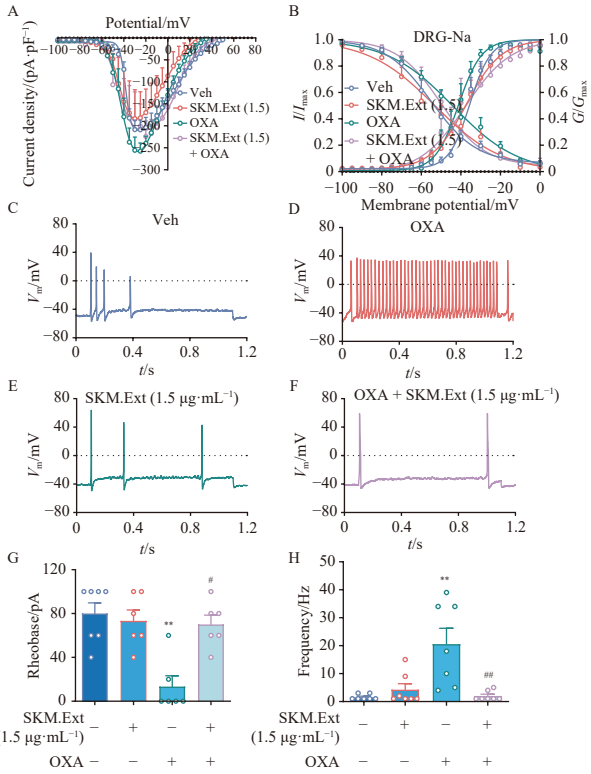

Fig. 6 SKM.Ext significantly mitigated OXA-induced hypersensitivity in DRG neurons. (A) Current–voltage (I–V) relationships of VGSC currents in DRG neurons under the following conditions: Veh, 100 μmol·L^{-1} OXA (24 h), 1.5 μg·mL^{-1} SKM.Ext (25 h), and 1.5 μg·mL^{-1} SKM.Ext pre-incubation (1 h) + OXA (24 h). (B) Steady-state activation and inactivation curves of VGSCs in the same treatment groups. Representative action potential firing induced by a 100-pA current injection in multiple spiking firing DRG neurons from (C) Veh, (D) 100 μmol·L^{-1} OXA (24 h), (E) 1.5 μg·mL^{-1} SKM.Ext (25 h), and (F) neurons preincubated with 1.5 μg·mL^{-1} SKM.Ext for 1 h followed by 100 μmol·L^{-1} OXA treatment for 24 h. (G) Quantification of rheobase in DRG neurons from Veh- and OXA-treated groups, with or without 1.5 1.5 μg·mL^{-1} SKM.Ext. n = 6–7. $^{**}P < 0.01$ *vs* Veh. $^{\#}P < 0.05$ *vs* OXA. (H) Quantification of firing frequency in DRG neurons from Veh- and OXA-treated groups, with or without 1.5 μg·mL^{-1} SKM.Ext. n = 7. $^{**}P < 0.01$ *vs* Veh. $^{\#\#}P < 0.01$ *vs* OXA. Data were analyzed using one-way ANOVA followed by Bonferroni's multiple comparisons test, with results shown as Mean ± SEM.

nerve injury [30]. In the Food and Drug Administration Adverse Event Reporting System (FAERS) database, 318 unique adverse events linked to OXA and classified under nervous system disorders were recorded. The most frequently reported neurological events included peripheral neuropathy, paresthesia, neurotoxicity, dizziness, dysarthria, tremor, and polyneuropathy [31]. Peripheral neuropathy is the most harmful side effect of OXA, often leading to treatment discontinuation and reduced quality of life in patients with various cancers [31]. OXA induces acute neuropathy characterized by cold-induced paresthesias and chronic neuropathy following cumulative doses of 540–850 mg·m^2 [32], associated with sensory and motor dysfunction involving glial activation, oxidative stress, and axonal degeneration [3]. Chronic neurotoxicity caused by OXA primarily affects the DRG, where oxidative stress may trigger apoptosis [33], leading to neuronal shrinkage and the development of OIPN. Given the positive correlation between DRG cell body size and axonal conduction velocity, neuronal atrophy may underlie the reduced sensory nerve conduction velocity observed in OIPN [34]. Although OXA treatment did not alter the total number of neurons in the L5 DRG, it significantly reduced neuronal diameter. In this study, both NAC, an oxidative stress inhibitor, and the SERCA2b agonists CDN and SKM.Ext significantly attenuated the reduction in DRG neuron diameter in OIPN. The critical role of ROS in OIPN was confirmed, and stimulation of SERCA2b was shown to markedly improve peripheral neuropathy. OXA also triggers allodynia through activation of proinflammatory cytokines such as TNF-α, IL-1, IL-6, and their associated receptors [35]. The SERCA agonists CDN and SKM.Ext significantly alleviated OXA-induced neuroinflammation in the DRG.

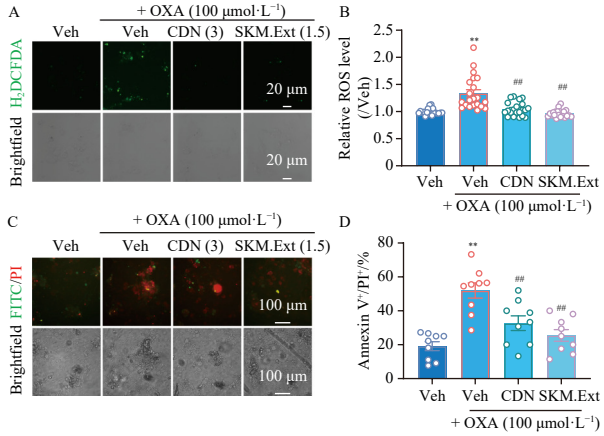

Fig. 7 CDN1163 and SKM.Ext significantly reduced OXA-induced oxidative stress and neuronal apoptosis/necrosis in DRG neurons. (A, B) 3 μmol·L^{-1} CDN1163 and 1.5 μg·mL^{-1} SKM.Ext significantly reduced 100 μmol·L^{-1} OXA-induced ROS in DRG neurons. (n = 21 DRG neurons from 7 different wells). Scale bar = 20 μm. $^{**}P < 0.01$ *vs* Veh group. $^{\#\#}P < 0.01$ *vs* OXA (100 μmol·L^{-1}, 12 h) + Veh group. (C, D) 3 μmol·L^{-1} CDN1163 and 1.5 μg·mL^{-1} SKM.Ext significantly reduced 100 μmol·L^{-1} OXA-induced neuronal apoptosis/necrosis in DRG neurons. Since Hoechst nuclear staining cannot distinguish satellite glial cells, (FITC$^+$/PI$^+$) × 100% / (round cells with diameters ranging from 10–50 μm in bright-field) = percentage of apoptotic/necrotic DRG neurons (n = 9). Scale bar = 100 μm. $^{**}P < 0.01$ *vs* Veh group. $^{\#\#}P < 0.01$ *vs* OXA (100 μmol·L^{-1}, 12 h) + Veh group. Data were analyzed using one-way ANOVA followed by Bonferroni's multiple comparisons test. Results are expressed as Mean ± SEM.

Neuropathic pain involves multiple molecular signaling pathways, including overexpression of VGSCs [14], inhibition of SERCA2b [8], and activation of transient receptor potential vanilloid 1 (TRPV1) channels in nociceptors [19]. Excessive activity of VGSCs and voltage-gated calcium channels (VGCCs) may contribute to chronic axonal damage, which is not surprising given that increased intracellular calcium is a well-documented contributor to axonal injury. A human study demonstrated that patients with OIPN exhibit heightened nerve excitability, evidenced by increased compound action potential amplitude, enhanced discharge, and variable intra-burst frequency [36]. While the precise mechanism underlying OXA-induced hyperexcitability remains unclear, one hypothesis suggests that oxalate, a metabolite of OXA, alters VGSC function by prolonging channel open state, thereby increasing sensory neuron excitability [4]. Additionally, tetrodotoxin (TTX) has been shown to block paclitaxel-induced mechanical and cold allodynia [23]. In the OIPN model, reduced SERCA2b expression in DRG neurons may lead to decreased ER calcium levels and elevated cytoplasmic calcium. Because Ca^{2+}/CaM-dependent phosphatase 2B dephosphorylates VGSCs, enhancing their current amplitude, whereas cAMP-dependent protein kinase phosphorylates VGSCs to promote membrane trafficking [37], downregulation of SERCA2b in DRG neurons may regulate VGSC current density *via* intracellular calcium modulation. Studies have identified a negative shift in the voltage dependence of Na^+ channel activation that could explain the hyperexcitability observed in acute OXA side effects [38]. Our research found that in DRG neurons incubated with 100 μmol·L^{-1} OXA for 24 h, VGSC current density increased, the steady-state activation curve shifted toward hyperpolarization, and the steady-state inactivation curve shifted toward depolarization, resulting in an enlarged window current. This leads to prolonged depolarizing currents and excessive Na^+ influx at resting membrane potential during OXA treatment, enhancing local depolarization and inducing action potential firing [39]. This mechanism likely contributes to the reduced action potential threshold and significantly increased firing frequency in OXA-treated DRG neurons. The SERCA agonists CDN and SKM.Ext reversed OXA-induced alterations in VGSCs in

DRG neurons. Because VGSCs mediate the depolarization phase of action potentials, the combination of CDN and SKM.Ext substantially mitigates OXA-induced sensitization of DRG neurons *in vitro*. These molecular mechanisms are likely involved in OIPN pathogenesis, and SERCA2b agonists may represent promising therapeutic candidates for OIPN.

Chemotherapy-induced peripheral neuropathy (CIPN) remains challenging to diagnose and manage. Various interventions have been explored in animal and human studies to alleviate symptoms by modulating oxidative stress, inflammatory cytokines, or ion channels. Amifostine, a prodrug with potent free radical scavenging properties, has demonstrated protective effects on normal tissues during chemotherapy and radiotherapy. Nausea, vomiting, transient hypotension, and allergic reactions were the most frequently reported adverse effects [40]. Its active form, WR-1065, effectively prevents OXA-induced neurotoxicity [30]. Ion channel inhibitors such as lidocaine have been reported to relieve CIPN. Intravenous lidocaine provides immediate pain relief and modulates sensitivity to cold and pinprick stimuli [41], particularly in acute cases, though its efficacy in chronic OIPN remains unestablished [42]. DLX, recommended by the American Society of Clinical Oncology (ASCO) for CIPN, alleviates neuropathic pain. Patients with OIPN may respond more favorably to DLX than those with paclitaxel-induced neuropathy, as suggested by exploratory data linking DLX's effects to distinct molecular pathways in OIPN [41]. However, DLX may cause side effects such as weight loss, nausea, and fatigue, potentially interfering with cancer treatment [43]. Venlafaxine, a second-generation serotonin-norepinephrine reuptake inhibitor, modulates neuronal activity by blocking the reuptake of serotonin and norepinephrine. Although a phase III double-blind randomized controlled trial demonstrated its benefit in reducing acute neurotoxicity and improving function in OXA-related neuropathy [44], a pilot study found it ineffective in preventing both acute and chronic symptoms [45]. Therefore, there is a pressing need for novel therapeutic strategies and targets for OIPN. Dysfunctional SERCA activity, leading to elevated intracellular calcium and ER stress, is implicated in cardiovascular and neurodegenerative diseases, making SERCA a compelling target for new therapies. However, enzyme-stimulating drugs are rare, and activating an enzyme is inherently more challenging than inhibiting it. Nevertheless, several compounds have been identified as SERCA activators, including CDN [27], CP-154526 [46], istaroxime [46] and Schekwanglupaside C [10]. In this study, the SKM.Ext formulation, which contains Schekwanglupaside C derived from *Schefflera kwangsiensis*, significantly mitigated OIPN, reversed the OXA-induced downregulation of SERCA2b in DRG neurons, and reduced neuronal hypersensitivity. Several key constituents of SKM.Ext (Table 1) exhibit anti-inflammatory, antioxidant, or analgesic properties that may collectively contribute to its efficacy against OIPN. Malic acid significantly alleviates primary fibromyalgia syndrome [47], while succinic acid suppresses inflammation and pain by inhibiting phospholipase A2 (PLA2) activity and arachidonic acid synthesis [48]. Fumaric acid demonstrates significant analgesic effects in the hot plate and tail flick tests [49]. Rhodioloside reduces LPS-induced TNF-α, IL-6, and IL-1β levels [50] and inhibits NLRP3 inflammasome activation and apoptosis, thereby mitigating inflammatory injury [51]. Compounds such as 4-hydroxybenzaldehyde [52], quercetin [53], rutin [54], and vanillin [55] exhibit both anti-inflammatory and antinociceptive activities. Syringaresinol achieves analgesia in OIPN by modulating spinal microglial inflammatory responses [56]. Sinapaldehyde exerts anti-inflammatory effects by suppressing reactive oxygen species and nitric oxide *via* COX-2 inhibition [57]. Additionally, naringenin limits OXA-induced DNA damage through its potent antioxidant effects [58]. Schekwanglupasides A and B [11], Schefflesides I, J, K, and L [59], and Schekwangsiensides K, N, L, and H [60] were isolated from SKM.Ext, although their bioactivities have not yet been reported. Collectively, these bioactive constituents may act synergistically to enhance the therapeutic efficacy of SKM.Ext in OIPN.

This finding may expand the clinical application of the traditional Chinese medicine Hantao Ye (*S. kwangsiensis*) in treating neurological disorders. SERCA2b activators represent a novel, mechanism-based therapeutic strategy for OIPN, with potential advantages in reducing oxidative stress, reversing neuronal hyperexcitability, correcting calcium dysregulation, and ultimately preventing neuronal apoptosis. However, due to the lack of human data and challenges in drug development, the clinical translation of SERCA activators remains limited. The safety and efficacy of SERCA2b activators require further investigation.

In conclusion, we propose the following: (1) OXA triggers oxidative stress, leading to reduced SERCA2b expression in DRG neurons. (2) This downregulation of SERCA2b contributes to elevated cytoplasmic Ca^{2+} levels. The increased intracellular Ca^{2+} may enhance Ca^{2+}-dependent facilitation of voltage-gated sodium channels (VGSCs), potentially through activation of protein kinases and phosphatases, thereby modulating VGSC membrane localization and gating kinetics [37]. (3) The resultant increase in Na^{+} current intensifies local membrane depolarization, promoting the generation and propagation of action potentials, which ultimately leads to DRG neuron hypersensitivity. Therefore, we hypothesize that the antioxidant NAC and SERCA agonists, such as CDN and SKM.Ext, may help prevent chronic OIPN by enhancing SERCA2b activity and restoring normal cytosolic Ca^{2+} homeostasis.

5. Conclusions

The current findings demonstrate that repeated administration of SERCA agonists, CDN, the antioxidant NAC, and SKM.Ext (an extract containing SERCA-activating lupane saponins), alleviates OXA-induced mechanical allodynia. This effect is mediated through enhanced SERCA2b expression in the L4–L6 DRG, accompanied by reduced expression of pro-inflammatory factors and attenuation of DRG neuronal hyperexcitability (Fig. 8). These outcomes suggest that SERCA agonists may represent a promising therapeutic strategy for OXA-induced neuropathy.

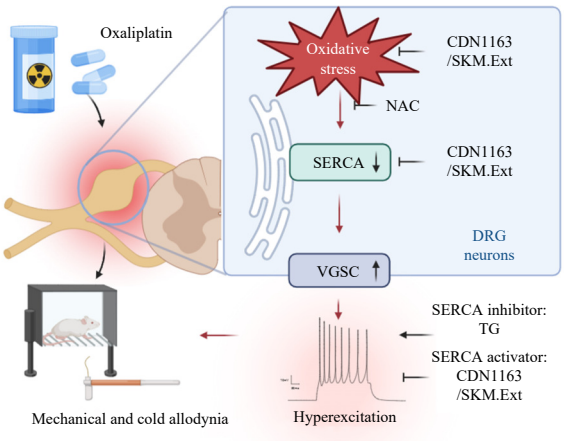

Fig. 8 Schematic illustration of SERCA2b in the regulation of mechanical and cold allodynia in OIPN rats. Repeated oxaliplatin (OXA) administration induces oxidative stress and neuroinflammation in dorsal root ganglion (DRG) neurons, leading to reduced expression of sarco/endoplasmic reticulum Ca^{2+}-ATPase 2b (SERCA2b) expression. Inhibition of SERCA2b by OXA increases voltage-gated sodium channel (VGSC) window currents, thereby enhancing DRG neuronal hyperexcitability and contributing to mechanical and cold allodynia. Thapsigargin (TG), a direct SERCA inhibitor, similarly augments neuronal hyperexcitability in DRG neurons. Pharmacological enhancement of SERCA2b function or expression with CDN1163 or SKM.Ext attenuates nerve injury, neuroinflammation, and neuronal hyperexcitability, effectively reversing OIPN-associated allodynia. Comparable protective effects are observed when oxidative stress is reduced by N-acetylcysteine (NAC). Created with BioRender.com.

Funding

This work was supported by the Natural Science Foundation of Jiangsu Province of China (No. BK20221054), the National Natural Science Foundation of China (Nos. 82204653, 82373929, and 82100585), the Major Program of Jiangsu Provincial Administration for Market Regulation (No. KJ2024014), "Double First-Class" University Project (No. CPU2022QZ30), the Open Fund Project of State Key Laboratory on Technologies for Chinese Medicine Pharmaceutical Process Control and Intelligent Manufacture (No. SKL2024Z0104), and Tibet Autonomous Region Science and Technology Plan Project Key Project (No. XZ202301ZY0014G).

Supporting information

Supporting information for this work can be obtained by contacting the corresponding authors *via* E-mail.

Declaration of competing interest

The authors declare that they have no known competing financial interests or personal relationships that could have appeared to influence the work reported in this paper.

References

1 Siegel RL, Giaquinto AN, Jemal A. Cancer statistics, 2024. *Ca-Cancer J Clin*. 2024;74(1):12-49. https://doi.org/10.3322/caac.21820.
2 Iragorri N, de Oliveira C, Fitzgerald N, et al. The out-of-pocket cost burden of cancer care—a systematic literature review. *Curr Oncol*. 2021;28(2):1216-1248. https://doi.org/10.3390/curroncol28020117.
3 Sałat K, Furgała A, Malikowska-Racia N. Searching for analgesic drug candidates alleviating oxaliplatin-induced cold hypersensitivity in mice. *Chem Biol Drug Des*. 2019;93(6):1061-1072. https://doi.org/10.1111/cbdd.13507.
4 Renn CL, Carozzi VA, Rhee P, et al. Multimodal assessment of painful peripheral neuropathy induced by chronic oxaliplatin-based chemotherapy in mice. *Mol Pain*. 2011;7:1744-8069-1747-1729. https://doi.org/10.1186/1744-8069-7-29.
5 Dahl R, Bezprozvanny I. SERCA pump as a novel therapeutic target for treating neurodegenerative disorders. *Biochem Bioph Res Commun*. 2024;734:150748. https://doi.org/10.1016/j.bbrc.2024.150748.
6 Duncan C, Mueller S, Simon E, et al. Painful nerve injury decreases sarco-endoplasmic reticulum Ca^{2+}-ATPase activity in axotomized sensory neurons. *Neuroscience*, 2013;231:247-257. https://doi.org/10.1016/j.neuroscience.2012.11.055.
7 Verkhratsky A, Fernyhough P. Mitochondrial malfunction and Ca^{2+} dyshomeostasis drive neuronal pathology in diabetes. *Cell Calcium*. 2008;44(1):112-122. https://doi.org/10.1016/j.ceca.2007.11.010.
8 Li SH, Zhao F, Tang QL, et al. Sarco/endoplasmic reticulum Ca^{2+}-ATPase (SERCA2b) mediates oxidation-induced endoplasmic reticulum stress to regulate neuropathic pain. *Brit J Pharmacol*. 2022;179(9):2016-2036. https://doi.org/10.1111/bph.15744.
9 Wang Y, Khan FA, Siddiqui M, et al. The genus *Schefflera*: a review of traditional uses, phytochemistry and pharmacology. *J Ethnopharmacol*. 2021;279:113675. https://doi.org/10.1016/j.jep.2020.113675.
10 Yang GL, Wang Y, Yu YY, et al. Schekwanglupaside C, a new lupane saponin from *Schefflera kwangsiensis*, is a potent activator of sarcoplasmic reticulum Ca^{2+}-ATPase. *Fitoterapia*. 2019;137:104150. https://doi.org/10.1016/j.fitote.2019.04.005.
11 Wang Y, Zhang CL, Liu YF, et al. Two new lupane saponins from *Schefflera kwangsiensis*. *Phytochem Lett*. 2016; 18:19-22. https://doi.org/10.1016/j.phytol.2016.08.021.
12 Kilkenny C, Browne W, Cuthill IC, et al. Animal research: reporting *in vivo* experiments—the ARRIVE guidelines. *Brit J Pharmacol*. 2011;31(4):991-993. https://doi.org/10.1038/jcbfm.2010.220.
13 McGrath JC, McLachlan EM, Zeller R. Transparency in research involving animals: The Basel Declaration and new principles for reporting research in BJP manuscripts. *Brit J Pharmacol*. 2015;172(10):2427-2432. https://doi.org/10.1111/bph.12956.
14 Zhao F, Tang QL, Xu J, et al. Dehydrocrenatidine inhibits voltage-gated sodium channels and ameliorates mechanic allodia in a rat model of neuropathic pain. *Toxins*. 2019;11(4):229. https://doi.org/10.3390/toxins11040229.
15 Wang RK, Yang TY, Feng Q, et al. Integration of network pharmacology and proteomics to elucidate the mechanism and targets of traditional Chinese medicine Biyuan Tongqiao granule against allergic rhinitis in an ovalbumin-induced mice model. *J Ethnopharmacol*. 2024;318:116816. https://doi.org/10.1016/j.jep.2023.116816.
16 Sakurai M, Egashira N, Kawashiri T, et al. Oxaliplatin-induced neuropathy in the rat: involvement of oxalate in cold hyperalgesia but not mechanical allodynia. *Pain*. 2009;147(1-3):165-174. https://doi.org/10.1016/j.pain.2009.09.003.
17 Yamamoto S, Ono H, Kume K, et al. Oxaliplatin treatment changes the function of sensory nerves in rats. *J Pharmacol. Sci*. 2016;130(4):189-193. https://doi.org/10.1016/j.jphs.2015.12.004.
18 Li L, Shao JP, Wang JS, et al. MiR-30b-5p attenuates oxaliplatin-induced peripheral neuropathic pain through the voltage-gated sodium channel $Na_v1.6$ in rats. *Neuropharmacology*. 2019;153:111-120. https://doi.org/10.1016/j.neuropharm.2019.04.024.
19 Zhao F, Wang SY, Li Y, et al. Surfactant cocamide monoethanolamide causes eye irritation by activating nociceptor TRPV1 channels. *Brit J Pharmacol*. 2021;178(17):3448-3462. https://doi.org/10.1111/bph.15491.
20 Wang Y, Sui YT, Lian AB, et al. PBX1 attenuates hair follicle-derived mesenchymal stem cell senescence and apoptosis by alleviating reactive oxygen species-mediated DNA damage instead of enhancing DNA damage repair. *Fron Cell Dev Biol*. 2021;9:739868. https://doi.org/10.3389/fcell.2021.739868.
21 Zimmermann M, Meyer N. Annexin V/7-AAD staining in keratinocytes. *Methods Mol Biol*. 2011;740:57-63. https://doi.org/10.1007/978-1-61779-108-6_8.
22 Dahl R. A new target for Parkinson's disease: small molecule SERCA activator CDN1163 ameliorates dyskinesia in 6-OHDA-lesioned rats. *Bioorgan Med Chem*. 2017;25(1):53-57. https://doi.org/10.1016/j.bmc.2016.10.008.
23 Aromolaran KA, Goldstein PA. Ion channels and neuronal hyperexcitability in chemotherapy-induced peripheral neuropathy: cause and effect? *Mol Pain*. 2017;13:1744806917714693.https://doi.org/10.1177/1744806917714693.
24 Frenz CT, Hansen A, Dupuis ND, et al. $Na_v1.5$ sodium channel window currents contribute to spontaneous firing in olfactory sensory neurons. *J Neurophysiol*. 2014;112(5):1091-1104. https://doi.org/10.1152/jn.00154.2014.
25 Wu B, Su XL, Zhang WT, et al. Oxaliplatin depolarizes the IB4–dorsal root ganglion neurons to drive the development of neuropathic pain through TRPM8 in mice. *Front Mol Neurosci*. 2021;14:690858. https://doi.org/10.3389/fnmol.2021.690858.
26 Kwak AW, Park JW, Lee SO, et al. Isolinderalactone sensitizes oxaliplatin-resistance colorectal cancer cells through JNK/p38 MAPK signaling pathways. *Phytomedicine*. 2022;105:154383. https://doi.org/10.1016/j.phymed.2022.154383.
27 Nguyen HT, Noriega Polo C, Wiederkehr A, et al. CDN1163, an activator of sarco/endoplasmic reticulum Ca^{2+} ATPase, up-regulates mitochondrial functions and protects against lipotoxicity in pancreatic β-cells. *Brit J Pharmacol*. 2023;180(21):2762-2776. https://doi.org/10.1111/bph.16160.
28 Du J, Sudlow LC, Luzhansky ID, et al. DRG explant model: elucidating mechanisms of oxaliplatin-induced peripheral neuropathy and identifying potential therapeutic targets. *bioRxiv*. 2023;10.05.560580. https://doi.org/10.1101/2023.10.05.560580.
29 Lin YT, Chen JC. Dorsal root ganglia isolation and primary culture to study neurotransmitter release. *J Vis Exp*. 2018;(140):57569. https://doi.org/10.3791/57569.
30 Mattar M, Umutoni F, Hassan MA, et al. Chemotherapy-induced peripheral neuropathy: a recent update on pathophysiology and treatment. *Life*. 2024;14(8):991. https://doi.org/10.3390/life14080991.
31 Pan XL, Xiao XT, Ding YL, et al. Neurological adverse events associated with oxaliplatin: a pharmacovigilance analysis based on FDA adverse event reporting system. *Front Pharmacol*. 2024;15:1431579. https://doi.org/10.3389/fphar.2024.1431579.
32 Kang LM, Tian YY, Xu SL. et al. Oxaliplatin-induced peripheral neuropathy: clinical features, mechanisms, prevention and treatment. *J Neurol*. 2021;268:3269-3282. https://doi.org/10.1007/s00415-020-09942-w.
33 Kanat O, Ertas H, Caner B. Platinum-induced neurotoxicity: a review of possible mechanisms. *World J Clin Oncol*. 2017;8(4):329. https://doi.org/10.5306/wjco.v8.i4.329.
34 Jamieson SMF, Liu J, Connor B, et al. Oxaliplatin causes selective atrophy of a subpopulation of dorsal root ganglion neurons without inducing cell loss. *Cancer Chemoth Pharm*. 2005;56:391-399. https://doi.org/10.1007/s00280-004-0953-4.
35 Avallone A, Bimonte S, Cardone C, et al. Pathophysiology and therapeutic perspectives for chemotherapy-induced peripheral neuropathy. *Anticancer Res*. 2022;42(10):4667-4678. https://doi.org/10.21873/anticanres.15971.
36 Basso M, Modoni A, Spada D, et al. Polymorphism of CAG motif of *SK3* gene is associated with acute oxaliplatin neurotoxicity. *Cancer Chemoth Pharm*. 2011;67:1179-1187. https://doi.org/10.1007/s00280-010-1466-y.
37 Shi HS, Lai K, Yin XL, et al. Ca^{2+}-dependent recruitment of voltage-gated sodium channels underlies bilirubin-induced overexcitation and neurotoxicity. *Cell Death Dis*. 2019;10(10):774. https://doi.org/10.1038/s41419-019-1979-1.
38 Broomand A, Jerremalm E, Yachnin J, et al. Oxaliplatin neurotoxicity–no general ion channel surface-charge effect. *J Negat Results Biomed*. 2009;8:1-8. https://doi.org/10.1186/1477-5751-8-2.
39 Pinet C, Le Grand B, John GW, et al. Thrombin facilitation of voltage-gated sodium channel activation in human cardiomyocytes: implications for ischemic sodium loading. *Circulation*. 2002;106(16):2098-2103. https://doi.org/10.1161/01.CIR.0000034510.64828.96.
40 King M, Joseph S, Albert A, et al. Use of amifostine for cytoprotection during radiation therapy: a review. *Oncology*. 2020;98(2):61-80. https://doi.org/10.1159/000502979.
41 Yang Y, Zhao B, Gao XJ, et al. Targeting strategies for oxaliplatin-induced peripheral neuropathy: clinical syndrome, molecular basis, and drug development. *J Exp Clin Cancer Res*. 2021;40:1-25. https://doi.org/10.1186/s13046-021-02141-z.
42 Kawashiri T, Mine K, Kobayashi D, et al. Therapeutic agents for oxaliplatin-induced peripheral neuropathy; experimental and clinical evidence. *Int J Mol Sci*. 2021;22(3):1393. https://doi.org/10.3390/ijms22031393.

43 Chen C, Xu JL, Gu ZC, et al. Danggui Sini decoction alleviates oxaliplatin-induced peripheral neuropathy by regulating gut microbiota and potentially relieving neuroinflammation related metabolic disorder. *Chin Med-Uk*. 2024;19(1):58. https://doi.org/10.1186/s13020-024-00929-7.

44 Durand JP, Deplanque G, Montheil V, et al. Efficacy of venlafaxine for the prevention and relief of oxaliplatin-induced acute neurotoxicity: results of EFFOX, a randomized, double-blind, placebo-controlled phase III trial. *Ann Onco*. 2012;23(1):200-205. https://doi.org/10.1093/annonc/mdr045.

45 Zimmerman C, Atherton PJ, Pachman D, et al. MC11C4: a pilot randomized, placebo-controlled, double-blind study of venlafaxine to prevent oxaliplatin-induced neuropathy. *Support Care Cancer*. 2016;24:1071-1078. https://doi.org/10.1007/s00520-015-2876-5.

46 Sordi G, Goti A, Young HS, et al. Stimulation of Ca^{2+}-ATPase transport activity by a small-molecule drug. *ChemMedChem*. 2021;16(21):3293-3299. https://doi.org/10.1002/cmdc.202100350.

47 Russell I, Michalek JE, Flechas JD, et al. Treatment of fibromyalgia syndrome with Super Malic: a randomized, double blind, placebo controlled, crossover pilot study. *J Rheumatol*. 1995;22(5):953-958.

48 Li JS, Su SL, Xu Z, et al. Potential roles of gut microbiota and microbial metabolites in chronic inflammatory pain and the mechanisms of therapy drugs. *Ther Adv Chronic Dis*. 2022;13:20406223221091177. https://doi.org/10.1177/20406223221091177.

49 Shakya A, Singh GK, Chatterjee SS, et al. Role of fumaric acid in anti-inflammatory and analgesic activities of a *Fumaria indica* extracts. *J Intercult Ethnopharmacol*. 2014;3(4):173. https://doi.org/10.5455/jice.20140912021115.

50 Guan S, Feng H, Song B, et al. Salidroside attenuates LPS-induced pro-inflammatory cytokine responses and improves survival in murine endotoxemia. *Int Immunopharmacol*. 2011;11(12):2194-2199. https://doi.org/10.1016/j.intimp.2011.09.018.

51 Liu J, Ma W, Zang CH, et al. Salidroside inhibits NLRP3 inflammasome activation and apoptosis in microglia induced by cerebral ischemia/reperfusion injury by inhibiting the TLR4/NF-κB signaling pathway. *Ann Transl Med*. 2021;9(22):1694. https://doi.org/10.21037/atm-21-5752.

52 Lim EJ, Kang HJ, Jung HJ, et al. Anti-Inflammatory, anti-angiogenic and anti-nociceptive activities of 4-hydroxybenzaldehyde. *Biomol Ther*. 2008;16(3):231-236. https://doi.org/10.4062/biomolther.2008.16.3.231.

53 Carullo G, Cappello AR, Frattaruolo L, et al. Quercetin and derivatives: useful tools in inflammation and pain management. *Future Med Chem*. 2017;9(1):79-93. https://doi.org/10.4155/fmc-2016-0186.

54 Azevedo MI, Pereira AF, Nogueira RB, et al. The antioxidant effects of the flavonoids rutin and quercetin inhibit oxaliplatin-induced chronic painful peripheral neuropathy. *Mol Pain*. 2013;9:53. https://doi.org/10.1186/1744-8069-9-53.

55 Kafali M, Finos MA, Tsoupras A. Vanillin and its derivatives: a critical review of their anti-inflammatory, anti-Infective, wound-healing, neuroprotective, and anti-cancer health-promoting benefits. *Nutraceuticals*. 2024;4(4):522-561. https://doi.org/10.3390/nutraceuticals4040030.

56 Lee JH, Choi JH, Kim J, et al. Syringaresinol alleviates oxaliplatin-induced neuropathic pain symptoms by inhibiting the inflammatory responses of spinal microglia. *Molecules*. 2022;27(23):8138. https://doi.org/10.3390/molecules27238138.

57 Baek SH, Park T, Kang MG, et al. Anti-inflammatory activity and ROS regulation effect of sinapaldehyde in LPS-stimulated RAW 264.7 macrophages. *Molecules*. 2020;25(18):4089. https://doi.org/10.3390/molecules25184089.

58 Ganaie MA, Jan BL, Khan TH, et al. The protective effect of naringenin on oxaliplatin-induced genotoxicity in mice. *Chem Pharm Bull*. 2019;67(5):433-438. https://doi.org/10.1248/cpb.c18-00809.

59 Wang CQ, Wang Y, Wang WJ, et al. New oleanane saponins from *Schefflera kwangsiensis*. *Phytochem Lett*. 2014;10:268-271. https://doi.org/10.1016/j.phytol.2014.10.010.

60 Wang Y, Liu YF, Zhang CL, et al. Four new triterpenoid saponins isolated from *Schefflera kwangsiensis* and their inhibitory activities against FBPase1. *Phytochem Lett* . 2016;15:204-209. https://doi.org/10.1016/j.phytol.2016.01.007.

61 Wang Y, Liang D, Khan FA, et al. Chemical constituents from *Schefflera leucantha* R. Vig. (Araliaceae). *Biochem Syst Ecol*. 2020;91:104076. https://doi.org/10.1016/j.bse.2020.104076.

62 Shen PL, Wang JJ. Quality analysis research of Chinese peach leaf. *J Hubei Univ Chin Med*. 2012;14(2):33-34. https://doi.org/10.3969/j.issn.1008-987x.2012.01.13.

63 Zhang L, Wang Y, Yu DQ. Simultaneous quantification of six major triterpenoid saponins in *Schefflera kwangsiensis* using high-performance liquid chromatography coupled to orbitrap mass spectrometry. *Nat Prod Res*. 2015;29(14):1350-1357.https://doi.org/10.1080/14786419.2015.1025397.

64 Yang T, Li XS, Zheng L, et al. Chemical Constituents of *Schefflera leucantha* (II). *J Chin Med Mater*. 2022;45(9):2118-2121. https://doi.org/10.13863/ j.issn1001-4454.2022.09.016.

65 Luo Y, Yan T, Gong ZP, et al. Research progress on chemical composition, pharmacological action and quality control of *Schefflera arboricola*. *Guizhou Agric Sci*. 2020;48(12):109-113. https://doi.org/10.3969/j.issn.1001-3601.2020.12.023.

66 Deng FS, Ma FX. Determination of the contents of two active components in *Schefflera kwangsiensis* Merr. Ex L. by RP-HPLC Method. *Jiangxi J Chin Tradit Med*. 2012;43(12):59-61.

67 Yang T, Li XS, Huang Y, et al. Chemical constituents from the stems and leafy stems of *Schefflera leucantha*. *J Chin Med Mater*. 2021;44(7):1631-1635. https://doi.org/10.13863/j.issn1001-4454.2021.07.016.

68 Yang X, Xu NZ, Fu WF, et al. Quality analysis of *Schefflera kwangsiensis* Merr. based on HPLC fingerprinting combined with chemometrics. *Herald Med*. 2024;43(2):267-273. https://doi.org/10.3870/j.issn.1004-0781.2024.02.019.